Lecture 1 Linear Elastic Fracture Mechanics: Basic Concepts (Small Scale Yielding: SSY)

Notation:

Components of vectors and tensors in 3D are indexed by *i, j, k*. Components of vectors and tensors in 2D are indexed by Greek letter such as α, β.

Summation convention of summing over repeated indices will be used throughout unless specified otherwise. We denote the position of a material point by its Cartesian coordinates x_i. The notation $_{,i}$ denotes partial derivative with respect to x_i.

Basic assumption: The solid is homogeneous, isotropic and linearly elastic in Lecture 1 and lecture 2. Small strain theory (where displacements, displacement gradients and rotations are assumed to be small) will be used throughout the first 2 lectures. I limit discussions to quasi-static problems and without loss of generality, assume zero body forces.

Review of Linear Elasticity

The basic equations of linear elasticity are:

The Cartesian component of the symmetric stress tensor σ_{ij} obeys

$$\sigma_{ij,j} = 0 \qquad \text{Force balance (no body forces, quasi-static)} \qquad (1)$$

The symmetric strain tensor ε_{ij} is related to the displacements of material points by

$$\varepsilon_{ij} = \frac{u_{i,j} + u_{j,i}}{2} \qquad \text{Kinematics} \qquad (2)$$

Finally, isotropic implies that

$$\varepsilon_{ij} = \frac{(1+\nu)\sigma_{ij}}{E} - \frac{\nu \sigma_{kk}}{E}\delta_{ij} \qquad \text{Constitutive model (generalized Hooke's law)} \qquad (3)$$

where *E* is the Young's Modulus and *v* is the Poisson's ratio. The shear modulus G is related to E and *v* by $2G = \frac{E}{1+\nu}$. The readers are reminded that elastomers are almost incompressible, with $\nu = 1/2, E = 3G$.

Crack tip Fields:

Figure 1 shows a *traction free* planar crack with a straight front in a specimen. To study the local fields, we extend the crack front to infinity and consider a semi-infinite crack (hence avoiding considering the stress field near the edge *E*, see Appendix). We then carry out an asymptotic or local analysis by assuming that the displacement field near the crack front has the following form:

$$u_i = Ar^s f_i(\theta)\ , \qquad r \to 0 \qquad (4)$$

where (r,θ,z) is a cylindrical coordinate with z axis coinciding with the crack front. We require the stress fields derived from (4) to satisfy the traction free boundary condition on the crack faces. The idea is simple: substitute (4) into (1-3) and enforces the appropriate traction free boundary conditions. After some messy calculations, we discover that in general there are three independent solutions. They are of the form:

$$\vec{u} = \underbrace{\frac{K_I}{2G}\sqrt{\frac{r}{2\pi}} f_\alpha^I(\theta)\vec{e}_\alpha}_{\vec{u}_I} + \underbrace{\frac{K_{II}}{2G}\sqrt{\frac{r}{2\pi}} f_\alpha^{II}(\theta)\vec{e}_\alpha}_{\vec{u}_{II}} + \frac{2K_{III}}{G}\sqrt{\frac{r}{2\pi}} f^{III}(\theta)\vec{e}_3 \qquad (5)$$

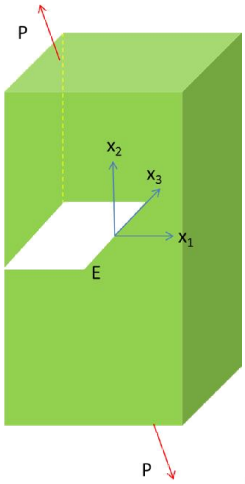

Figure 1: Geometry of a planar crack in a 3D specimen, the point E is the vertex where the crack front intersects the free surface (see discussion in Appendix regarding the local fields at E)

The three independent scalars K_I, K_{II} and K_{III} are called Mode I, II and III stress intensity factors respectively (units = *stress* $\times\sqrt{length}$). They cannot be determined by asymptotic or local analysis. Their values depend on the manner of loading and specimen geometry. For complicated geometries, their values will vary along the crack front, and they can only be determined by numerical methods. For simple geometries, they can be found in [1].

The functions $f_\alpha^I(\theta)$, $f_\alpha^{II}(\theta)$ and $f_3^{III}(\theta)$ are *universal* functions describing the angular variations of these local fields, they are found to be [2]:

$$\begin{Bmatrix} f_1^I \\ f_2^I \end{Bmatrix} = \begin{Bmatrix} \cos(\theta/2)\left[\kappa - 1 + 2\sin^2(\theta/2)\right] \\ \sin(\theta/2)\left[\kappa + 1 - 2\cos^2(\theta/2)\right] \end{Bmatrix} \qquad \text{Mode I} \qquad (6)$$

$$\begin{Bmatrix} f_1^{II} \\ f_2^{II} \end{Bmatrix} = \begin{Bmatrix} \sin(\theta/2)\left[\kappa + 1 + 2\cos^2(\theta/2)\right] \\ -\cos(\theta/2)\left[\kappa - 1 - 2\sin^2(\theta/2)\right] \end{Bmatrix} \qquad \text{Mode II} \qquad (7)$$

$$f^{III} = \sin(\theta/2), \qquad \text{Mode III} \qquad (8)$$

where $\kappa = 3 - 4\nu$.

Here are some important points:

1. The displacement fields corresponding to Mode I is symmetric, that is,

$$u_1^I(x_1, x_2) = u_1^I(x_1, -x_2), u_2^I(x_1, x_2) = -u_2^I(x_1, -x_2) \qquad (9)$$

In particular, on the crack faces $\theta = \pm\pi$, the crack opens symmetrically, the crack opening displacement (COD) is:

$$COD = u_2^I(r, \theta = \pi) - u_2^I(r, \theta = -\pi) = \frac{[\kappa + 1]}{G} K_I \sqrt{\frac{r}{2\pi}} \qquad (10)$$

2. The displacement fields corresponding to Mode II is anti-symmetric, that is:

$$u_1^{II}(x_1, x_2) = -u_1^{II}(x_1, -x_2), u_2^{II}(x_1, x_2) = u_2^{II}(x_1, -x_2) \qquad (11)$$

In Mode II, the crack does not open, the crack faces slide pass each other, and the relative slip on the crack face is

$$u_1^I(r, \theta = \pi) - u_1^I(r, \theta = -\pi) = \frac{[\kappa + 1]}{G} K_{II} \sqrt{\frac{r}{2\pi}} \qquad (12)$$

Likewise, in Mode III, the crack faces slide pass each other in the out of plane direction, the relative slip is:

$$u_3^{III}(r, \theta = \pi) - u_3^{III}(r, \theta = -\pi) = \frac{4K_{III}}{G} \sqrt{\frac{r}{2\pi}} \qquad (13)$$

Thus, local analysis shows that the displacement fields near the crack tip can be described by the superposition of three different modes of relative displacements of the crack faces.

3. The near tip displacements have the *universal* form given by (5-8), *irrespectively of the specimen geometry and the manner of loading*. The displacement fields are directly proportional to the square root of the distance from the crack tip. Its magnitude is controlled by three scalar parameters - the stress intensity factors.

Since the stress fields are related linearly to the strains, and the strains are gradients of the displacements, the local stresses must be proportional to $1/\sqrt{r}$, that is, they become unbounded as the crack tip is approached. Using (6), (7) and (8), after some algebra, the *in-plane* stresses are given by [2]:

$$\begin{Bmatrix}\sigma_{11}\\ \sigma_{12}\\ \sigma_{22}\end{Bmatrix} = \frac{K_{\mathrm{I}}}{(2\pi r)^{1/2}}\cos(\theta/2)\begin{Bmatrix}1-\sin(\theta/2)\sin(3\theta/2)\\ \sin(\theta/2)\cos(3\theta/2)\\ 1+\sin(\theta/2)\sin(3\theta/2)\end{Bmatrix} \tag{14a}$$

$$\begin{Bmatrix}\sigma_{11}\\ \sigma_{12}\\ \sigma_{22}\end{Bmatrix} = \frac{K_{\mathrm{II}}}{(2\pi r)^{1/2}}\begin{Bmatrix}-\sin(\theta/2)\,[2+\cos(\theta/2)\cos(3\theta/2)]\\ \cos(\theta/2)\,[1-\sin(\theta/2)\sin(3\theta/2)]\\ \sin(\theta/2)\cos(\theta/2)\cos(3\theta/2)\end{Bmatrix} \tag{14b,c}$$

$$\begin{Bmatrix}\sigma_{13}\\ \sigma_{23}\end{Bmatrix} = \frac{K_{\mathrm{III}}}{(2\pi r)^{1/2}}\begin{Bmatrix}-\sin(\theta/2)\\ \cos(\theta/2)\end{Bmatrix}$$

It should be noted that the deformation and stress fields given in Mode I and Mode II above can be obtained by solving a *2 dimensional plane strain* crack problem, whereas the Mode III solution can be obtained by solving an *2 dimensional anti-plane* shear problem.

Recall, in plane strain deformation, the out of plane displacement u_3 is exactly zero; as a result,

$$\sigma_{31}=\sigma_{32}=0 \quad \text{and} \quad \sigma_{33}=\nu\left(\sigma_{11}+\sigma_{22}\right) \tag{15}$$

Thus, directly ahead of the crack tip ($\theta=0$) of a Mode I crack, the near tip stress state is *hydrostatic* for an *incompressible* solid. Specifically,

$$\theta=0,\nu=1/2\Rightarrow\sigma_{33}=\sigma_{11}=\sigma_{22}=\frac{K_I}{\sqrt{2\pi r}} \tag{16}$$

It is well known that plastic flow does not occur readily under hydrostatic stress, therefore, the plastic zone size (e.g. in metal) are usually quite small directly ahead of the crack tip. On the other hand, for elastomers, a hydrostatic stress state is known to favor nucleation of cavities.

The stress fields given by (14a,b) are also valid for plates subjected to in plane loading (no bending). These results can be obtained by plane stress analysis where the out of plane stress components σ_{3i} are assumed to be identically zero. Note that the in-plane stresses of a plane stress specimen (plate) is identical to that of a plane strain specimen - they are both given by (14a,b). The in-plane displacement fields are given by the first two terms of (5) provided that κ changes to $(3-\nu)/(1+\nu)$.

The elastic solution predicts that the stress and strain field is infinite as one approaches the crack tip. Since no material can support infinite stress (besides, linear elasticity assumes small strains, so the theory is no longer correct near the crack tip), the elastic solution cannot be valid all the way to the crack tip. The basis of LEFM is based on the *Small Scale Yielding* (SSY) assumption. Here is how Rice [3] describes it:

"The utility of elastic stress analyzes lies in the similarity of near crack tip stress distributions for all crack configurations. Presuming deviation from linearity to occur only over a region that is small compared to

geometrical dimensions (small-scale yielding), the elastic stress-intensity factor controls the local deformation field. This is the sense that two bodies with cracks of different size and with different manners of load applications, but which are otherwise identical, will have identical near tip deformation fields if the stress intensity factors are equal. Thus, the stress intensity factors uniquely characterizes the load sensed at the crack tip in situations of small-scale yielding, and criteria governing crack extension for a given local load rate, temperature, environment, sheet thickness (when plane stress fracture modes are possible), and history of prior deformation may be expressed in terms of stress intensity factors….."

The story is more involved than what's described above. For example, after substituting (4) into (1-3), you will discover three boundary value problems involving ordinary differential equations for the angular distribution functions f_α with *s* as an eigenvalue. In general, there are infinitely many eigenvalues (hence infinitely many eigenfunctions) that satisfies the traction free boundary conditions. The standard approach is to select the eigenvalue that give the *weakest* singularity (which turns out to be -½). The question is why we neglect these higher order singularities.

Since this idea is frequently passed over in fracture mechanics textbooks, I will illustrate it by considering Mode III. A detail description of this idea can be found in [3]. Since we are interested in local fields, we consider first the problem of a semi-infinite crack lying on the negative x_1 axis, with its tip at the origin. For anti-plane shear there is only one non-trivial displacement field, namely, $u_1 = u_2 = 0, u_3 = w\left(x_1, x_2\right)$. Using this assumption, one can show that all the in plane stress components and σ_{33} vanish with the exception of σ_{31} and σ_{32} which depend only on the in-plane coordinates. The governing equation is particularly simple, it is

$$\nabla^2 w = 0 \qquad (17)$$

where ∇^2 is the two dimensional Laplacian operator. The traction free boundary condition for a Mode III crack reduces to

$$\sigma_{32}(r, \theta = \pm\pi) = 0 \Rightarrow w_{,2}\left(r, \theta = \pm\pi\right) = 0 \qquad (18)$$

Substituting $w = r^s f\left(\theta\right)$ into (17) give rise to the following boundary value problem:

$$\frac{d^2 f}{d\theta^2} + s^2 f = 0 \qquad \frac{df}{d\theta}\left(\theta = \pm\pi\right) = 0 \qquad (19a,b)$$

The only anti-symmetric solution (since we physically expect that w = 0 for $\theta = 0$) that satisfy (19a) has the form:

$$f\left(\theta\right) = A\, sin\left(s\theta\right) \qquad (20)$$

where *A* is an arbitrary constant. For a non-trivial solution that satisfies the boundary condition (19b), we must have

$$\cos(s\pi) = 0 \tag{21}$$

This means that the eigenvalues are:

$$s = \frac{2n+1}{2} \qquad \text{for } \textit{any integer } n \tag{22}$$

The corresponding eigenfunctions are

$$f_n(\theta) = A_n \sin\left(\frac{2n+1}{2}\theta\right) \tag{23}$$

Note that the stress field given in (14c) corresponds to s = ½ (n= 0). The stress fields corresponding to each eigenvalue can be obtained using the constitutive law $\sigma_{3\alpha} = Gw_{,\alpha}$. For convenience, we express the Cartesian stress components of $\sigma_{3\alpha} = Gw_{,\alpha}$ into their polar components. A simple calculation shows that

$$\begin{aligned} \tau_r &\equiv \sigma_{31}\cos\theta + \sigma_{32}\sin\theta = Gw_{,r} \\ \tau_\theta &\equiv \sigma_{32}\cos\theta - \sigma_{31}\sin\theta = G\frac{w_{,\theta}}{r} \end{aligned} \tag{24}$$

Thus, the near tip stress fields in polar coordinates are of the form:

$$\begin{pmatrix} \tau_r^n \\ \tau_\theta^n \end{pmatrix} = b_n r^{\frac{2n-1}{2}} \begin{pmatrix} \sin\left(\frac{2n+1}{2}\theta\right) \\ \cos\left(\frac{2n+1}{2}\theta\right) \end{pmatrix}, \quad b_n = \frac{2n+1}{2} G A_n \tag{25}$$

In a similar way, one can show that there are infinitely many eigenvalues and eigenfunctions for plane strain Mode I and II cracks (this is also true for interface cracks in elastic materials). Since each of these functions satisfies (17) and the traction free boundary condition, by linearity, any linear combination of them is also a solution near the crack tip. Therefore, one would expect the full expansion of the stress field near the crack tip should have the form:

$$\begin{pmatrix} \tau_r \\ \tau_\theta \end{pmatrix} = \begin{pmatrix} \sum_{n=-\infty}^{\infty} b_n r^{\frac{2n-1}{2}} \sin\left(\frac{2n+1}{2}\theta\right) \\ \sum_{n=-\infty}^{\infty} b_n r^{\frac{2n-1}{2}} \cos\left(\frac{2n+1}{2}\theta\right) \end{pmatrix} \tag{26}$$

Equation (28) shows that there are *infinitely many terms with higher singularity* than the *n = 0* term.

The question is: why do we only select the *n* = 0 term (with an inverse square root singularity) despite the fact that there are infinitely many other terms that are more singular (and therefore

presumably more *dominant* as *r* approaches zero)? The standard arguments for keeping only the n = 0 term are:

(i) The strain energy in the crack tip region must be bounded
(ii) The displacement in the crack tip region must be bounded
(iii) Uniqueness of elastic solution is lost if higher order solution are allowed
(iv) The solution for the stress in the vicinity of an elliptic hole, in the limit of the aspect ratio goes to infinity, does not have such higher order singularities.

These are all flaw reasons. For example, (i) and (ii) above are violated by many solutions in linear elasticity that are used to represent physical phenomena. Examples include: a line load on the surface of a half space, a point load in a full space, and a dislocation in full space. All these solution has unbounded energy and the first two has unbounded displacements. The displacement and energy singularities are not problematic in these solutions, because the solutions are not assumed to be applicable all the way to singularity point. Rather, the solution is used only at distances that are large compared to the region over which the model (a load with no spatial extent and linear elastic behavior) is invalid. The same idea applies to fracture mechanics. Since no real material remains linear elastic when subjected to sufficiently large stresses, and no material can bear infinite stress or strains, there must be some region Ω surrounding the crack tip where the material behavior and changes in geometry deviates significantly from the prediction of linear elasticity. Inside Ω, which we called the process zone, the material behavior can be nonlinear, material surfaces may separate, voids and microcracks can nucleate and grow, continuum solution may not even be accurate etc.); outside this region, where linear elasticity is accurate, there is no singularity. Thus solutions that would have infinite displacement or energy if evaluated at the crack tip are not supposed to be used at the crack tip. In other words, the standard arguments about bounded displacement or strain energy do not legitimately rule out these higher order singular terms because these arguments make use of the linear elastic solution in a region where the solution is *a priori* known to be invalid.

The uniqueness assumption (iii) is also not justified. Since the strain energy is bounded outside the process zone Ω, the uniqueness condition (iii) is satisfied in the elastic region D which consists of material outside Ω, whether or not terms with higher order singularities are in the series description of the elastic field. Whether or not an entire fracture problem has a unique solution then depends on the material behavior inside the process zone. Uniqueness, if assumed to be valid for unknown material models in the process zone, is an additional postulate.

Finally, although one way of getting a flat or perfectly sharp crack is as the limit of an infinite aspect ratio elliptical hole (iv), a real crack is not necessarily well described by this limit. A mathematically sharp crack, if that is what one chooses to study, may be found as the limit of any number of non-singular fields. Many such limits lead to high order singularities in the limit of zero nonlinear zone size. For example, a cohesive zone model with both tensile and compressive stresses which goes appropriately to infinity as the cohesive zone size is reduced will lead to a traction free crack solution that does have high order singularities (see Lecture 2).

Having accepted at least the possibility of existence of these higher order singularities (which we shall demonstrate below), we need to reexamine the SSY condition where it is assumed that there is a region near the crack tip (but outside the process zone) where the K field dominates (despite the fact that there are infinitely many terms in the series that are more singular). *In fact, it is not sufficient that such a region exist, but that all specimens that satisfy SSY must share a common region surrounding the crack tip where K dominates*. Indeed, one naturally assumes that if the stresses are accurately known on the boundary of region that enclosed the crack tip, then the full (nonlinear material behavior, finite deformation etc.) stress and deformation fields inside the region can be determined by solving an appropriate boundary value problem. That is, one assumes that some kind of uniqueness assumption does hold for the crack tip material. To ensure the same local crack tip solution for two different specimens, the two crack tip regions associated with the specimens have to be effectively loaded by the same boundary conditions. Thus, any pair of bodies of identical material composition for which K is used to characterize fracture should have interior surface *at the same distance from the crack tip* where the stress field is dominated by the K field. To summarize, the SSY condition depends on the following conditions:

- the K field given by (14a,b,c) is dominant over all singular and non-singular terms in the series expansion (e.g. (26) for Mode III cracks), in some annular region surrounding the crack tip outside Ω .
- Specimens which are compared using SSY must have region of K dominance which has non-zero intersection. Thus, a radius r_K exists so that the K field dominates the stress field on all such specimens at r_K . This situation is illustrated for two specimens in Figure 2.

Some researchers have attempted to improve the accuracy of the stress field near the crack tip using a series expansion that ignored the existence of these higher order singular terms, e.g. in Mode I,

$$\sigma_{ij} = \frac{K_I}{\sqrt{2\pi}} r^{-1/2} \hat{\sigma}^I_{ij}(\theta,0) + a_1 r^{1/2} \hat{\sigma}^I_{ij}(\theta,1) + ... + a_m r^{m-1/2} \hat{\sigma}^I_{ij}(\theta,m) + ... \qquad (27)$$

where $\hat{\sigma}^I_{ij}(\theta,m)$ are the eigenfunctions associated with the different eigenvalues describing the angular distribution of the stress fields. These eigenfunctions are universal functions independent of specimen geometry. However, if the higher order terms exist outside the process zone, any attempt to estimate or to calculate the a_m 's in (27) is not only futile but incorrect as infinitely many terms with m < -1 are thus neglected.

Let us again demonstrate this idea using a Mode III crack. Figure 3 shows a finite specimen loaded under antiplane shear condition. The crack tip is located at (x_1=x = 0, x_2=y = 0) and the process zone Ω is assumed to be sufficiently small so that it does not completely engulf the crack length. Let (r,θ) be a polar coordinate system attached to the crack tip. The term process zone means that inside this zone one or more of the usual assumptions regarding small strain linearity elasticity break down. Outside Ω linear elasticity is assumed to be exactly satisfied. The problem is shown in Fig. 3a, where C_1 and C_2 are circular boundaries enclosing the crack tip region. Between the circles, the material is purely linear

elastic. Thus we may consider the purely linear elastic problem in Figure 3b. The radius of C_1, ρ is chosen to be as small as possible with Ω still being contained in C_1; that is, ρ is the outermost extent of Ω. The radius of C_2 is *R*, it is larger than ρ, and is chosen to be as large as possible while still contain in the specimen. The traction τ_r on these boundaries is assumed to be bounded so that

$$\tau_r(R,\theta) = \tau_a F(\theta) \qquad (\textit{Outer boundary})$$
$$\tau_r(\rho,\theta) = \tau_0 H(\theta) \qquad (\textit{inner boundary}) \qquad (28a,b)$$

where τ_a and τ_0 are reference stresses defined by the maximum value of the tractions on the circles respectively. We shall assume that each of these prescribed tractions is separately self-equilibrated. Physically, one may think of τ_a as a scalar measure of the level of the applied load on the boundary of the specimen and τ_0 as a scalar measure of the inelastic stress at the outer boundary of the process zone Ω. For any actual specimen and confined process zone our replacement problem is exactly coincident with the solution to the original problem. Thus, the original singular and possibly nonlinear problem is reduced to the solution of a bounded linear problem.

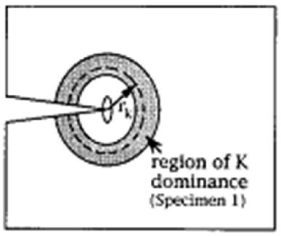

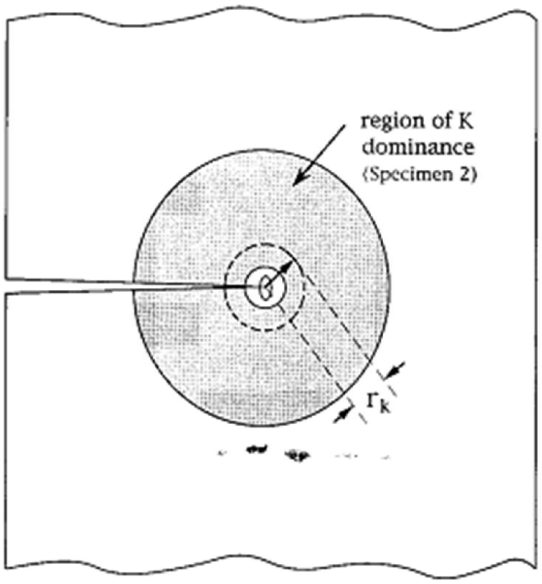

Figure 2: Two different specimens (I and II) made of the same material are shown. The region in which K field dominates is shaded in both cases. In order for the two specimens has the same fracture behavior, it is necessary that there exist a radius r_k that is the region of K dominance region for both specimen. The *same* elliptical region Ω at the crack tips represents a region where linear elasticity breaks down (they should be identical in shape and size if r_k exists).

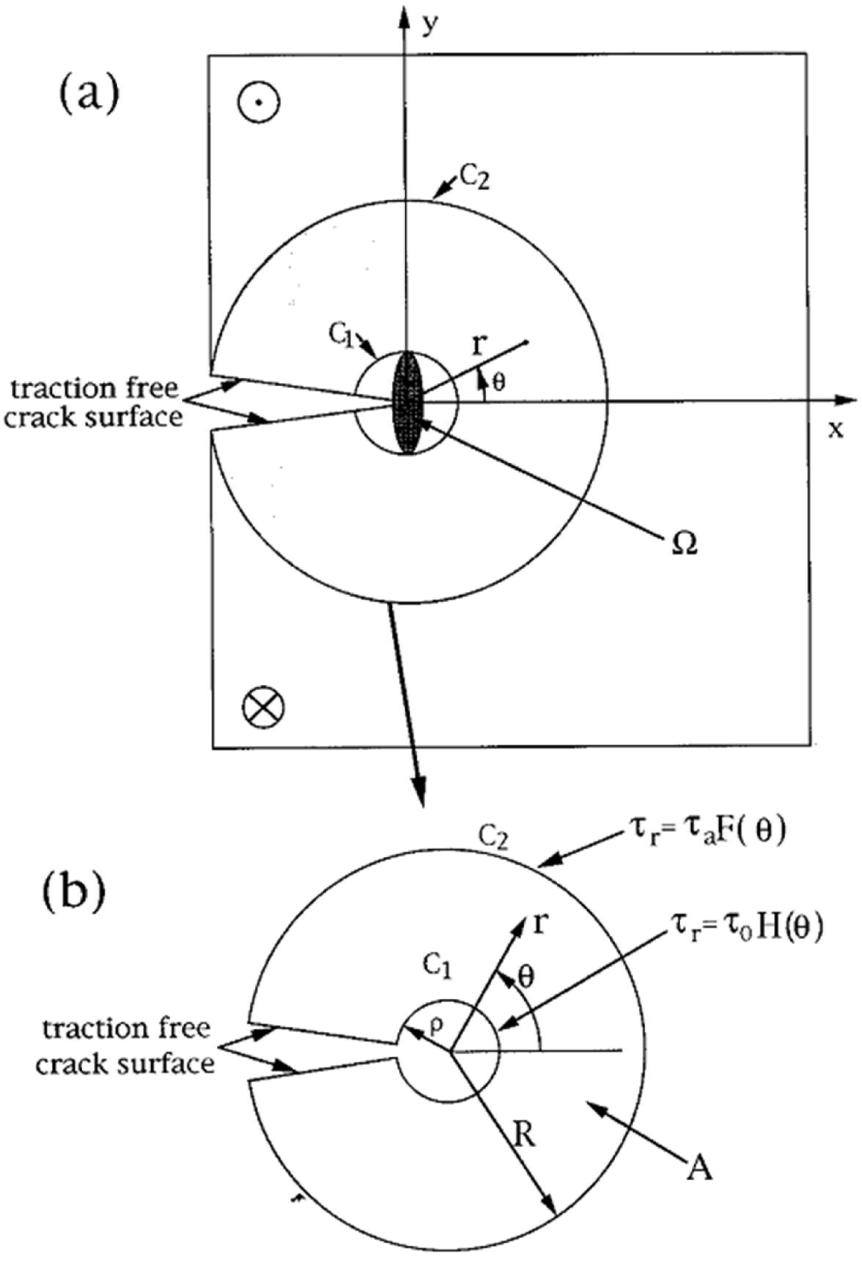

Figure 3a shows a specimen with two circles drawn. The inner circle is the small circle that can be drawn that completely encloses the nonlinear process zone, denoted by Ω . The material outside the inner circle C_1 (radius ρ) is homogeneous, isotropic and linearly elastic. The radius of the outer circle C_2

is R and is chosen so that R > ρ and is as closed as possible to the specimen dimensions. (b)shows our replacement for the specimen in Fig. 3a. A specimen is considered in the region A that lies between the two circles. The tractions on these circular boundaries are the same as those occurring in the original specimen at the same locations.

Our approach is to first determine the stress field inside the region $A=\{\rho<r<R,-\pi<\theta<\pi\}$ in Figure 3b. This can be done by solving (17) subjected to boundary conditions (28a,b) and the traction free boundary condition

$$\tau_r\left(\rho<r<R,\theta=\pm\pi\right)=0 \qquad (28c)$$

on the crack faces. Closed form solution of (17) subjected to the boundary conditions (28a,b,c) is given as sum of two fields labelled I (inner surface traction free), O (outer surface traction free). Here I only state the result for the anti-symmetric case, which is of greatest interest to fracture. Details as well as the symmetric case can be found in [4].

$$\begin{pmatrix}\tau_r\\ \tau_\theta\end{pmatrix}=\tau_a\begin{pmatrix}\tau_r^I+\tau_r^O\\ \tau_\theta^I+\tau_\theta^O\end{pmatrix} \qquad (29a)$$

$$\begin{aligned}
\tau_r^I &= \sum_{n=0}^{\infty} b_n^I\left(r/R\right)^{(2n-1)/2}\left[1-\left(\rho/r\right)^{2n+1}\right]sin\left(\frac{(2n+1)\theta}{2}\right)\\
\tau_\theta^I &= \sum_{n=0}^{\infty} b_n^I\left(r/R\right)^{(2n-1)/2}\left[1+\left(\rho/r\right)^{2n+1}\right]cos\left(\frac{(2n+1)\theta}{2}\right)\\
\tau_r^O &= \frac{1}{\mu}\sum_{n=0}^{\infty}\varepsilon^{(2n+3)/2} b_n^{II}\left(r/R\right)^{(2n-1)/2}\left[1-\left(R/r\right)^{2n+1}\right]sin\left(\frac{(2n+1)\theta}{2}\right)\\
\tau_\theta^O &= \frac{1}{\mu}\sum_{n=0}^{\infty}\varepsilon^{(2n+3)/2} b_n^{II}\left(r/R\right)^{(2n-1)/2}\left[1+\left(R/r\right)^{2n+1}\right]cos\left(\frac{(2n+1)\theta}{2}\right)
\end{aligned} \qquad (29b\text{-}e)$$

where

$$\varepsilon\equiv\rho/R,\quad \mu\equiv\tau_a/\tau_0 \qquad (29f)$$

and

$$\begin{aligned}
b_n^I &= \frac{F_n}{1-\varepsilon^{2n+1}},\quad F_n=\frac{1}{\pi}\int_{-\pi}^{\pi}F(\theta)\,sin\left(\frac{2n+1}{2}\theta\right)d\theta,\\
b_n^{II} &= \frac{-H_n}{1-\varepsilon^{2n+1}},\quad H_n=\frac{1}{\pi}\int_{-\pi}^{\pi}F(\theta)\,sin\left(\frac{2n+1}{2}\theta\right)d\theta
\end{aligned} \qquad (29g,h)$$

Note that the functions τ_r^I,τ_r^O etc. are dimensionless. Also $\varepsilon\equiv\rho/R<1$ and b_n^I , b_n^{II} are order one terms since both F and H are less than equal to 1. $\left(\tau_r^I,\tau_\theta^I\right)$ is the stress field if traction is applied on the

outer circle and no traction is applied on the inner circle whereas $\left(\tau_r^O, \tau_\theta^O\right)$ is the stress field if traction is applied on the inner circle and no traction is applied on the outer boundary. Note that the series solution is exact and consists of terms that are fractional powers of *r* and there is displacement discontinuity across the crack faces.

The results given by (29) above established that all the terms involving higher order singularities (i.e., second terms in square brackets in 29b-e) are present in the annular region A . Note that the coefficient of the *n* = 0 term in (29b-d) is related to the Mode III stress intensity factor K_{III} by

$$K_{III} = \left[\frac{1-\left(H_0 / F_0\right)\varepsilon^{3/2}\mu^{-1}}{1-\varepsilon}\right]\underbrace{\sqrt{2\pi R}\tau_a F_0}_{K_{III}^{applied}} \tag{30a}$$

where

$$K_{III}^{applied} = \sqrt{2\pi R}\tau_a F_0 \tag{30b}$$

is the usual stress intensity factor, namely, the strength of the inverse square root singularity in specimen with a perfectly sharp structureless crack. Recall that (see (29g,h)) H_0, F_0 are order one terms and μ^{-1} is the ratio of the stress in the nonlinear zone to the applied traction on the outer boundary. Since we have not yet explicitly made any assumptions about material behavior in the process zone, quantities such as τ_0 , ρ, μ, ε are as yet unrelated.

If SSY is valid, the size of the process zone must be governed by K_{III} and τ_0 . A dimensional argument requires that ρ must be proportional to K_{III}^2 / τ_0^2 . By (30a), K_{III} is approximately proportional $\tau_a\sqrt{R}$, we have

$$\varepsilon = C\mu^2 \tag{31}$$

where C is a positive dimensionless function of ε and is of order one. We can rewrite (30a) as

$$K_{III} = \left[\frac{1-C\varepsilon}{1-\varepsilon}\right]K_{III}^{applied} \tag{32}$$

where constants of order one were absorbed in C. As expected, only if the process zone is small in comparison with typical specimen dimensions, i.e., $\varepsilon = \rho / R << 1$ is the actual stress intensity factor K_{III} well approximated by the applied stress intensity factor $K_{III}^{applied}$.

Let us now examine the order of magnitude of each term in the series of in the annulus region A' defined by

$$A' = \left\{ \left(r,\theta\right), r = \varepsilon^{\lambda} R, 1 > \lambda > 0 \right\} \tag{33}$$

Note that A' is contain in A. The series solution can now be written in terms of $\varepsilon^{\lambda} R$. Let us first look at τ_{θ}^{I} (similar result applies to the other component)

$$\begin{aligned}
\tau_{\theta}^{I}\left(r = \varepsilon^{\lambda} R\right) &= \sum_{n=0}^{\infty} b_n^{I} \varepsilon^{\lambda(2n-1)/2} \left[1 + \varepsilon^{(2n+1)(1-\lambda)}\right] cos\left(\frac{\left(2n+1\right)\theta}{2}\right) \\
&= \sum_{n=0}^{\infty} b_n^{I} \varepsilon^{\lambda(2n-1)/2} cos\left(\frac{\left(2n+1\right)\theta}{2}\right) + \sum_{n=0}^{\infty} b_n^{I} \varepsilon^{(2n-1)/2} \left[\varepsilon^{(1-\lambda)}\right]^{(2n+3)/2} cos\left(\frac{\left(2n+1\right)\theta}{2}\right) \\
&= \ldots + \underbrace{b_1^{I} \varepsilon^{\lambda/2}}_{r^{1/2}} cos\left(\frac{3\theta}{2}\right) + \underbrace{b_0^{I} \varepsilon^{-\lambda/2}}_{r^{-1/2}} cos\left(\frac{\theta}{2}\right) + \underbrace{b_0^{I} \varepsilon^{-\lambda/2+3(1-\lambda)/2}}_{r^{-3/2}} cos\left(\frac{\theta}{2}\right) + \ldots\ldots
\end{aligned} \tag{34}$$

Examination of the terms in (34) reveals that the $r^{-1/2}$ has the smallest power in ε which is $\varepsilon^{-\lambda/2}$, thus in dominates over all other terms of the series (singular or non-singular) in A' in the limit as ε goes to zero.

Let us now apply the same procedure to τ_{θ}^{O}, the arrangement is:

$$\begin{aligned}
\tau_{\theta}^{O} &= \frac{1}{\mu} \sum_{n=0}^{\infty} \varepsilon^{(2n+3)/2} b_n^{II} \left(\varepsilon^{\lambda}\right)^{(2n-1)/2} cos\left(\frac{\left(2n+1\right)\theta}{2}\right) + \frac{1}{\mu} \sum_{n=0}^{\infty} \varepsilon^{(2n+3)/2} b_n^{II} \left(\varepsilon^{-\lambda}\right)^{(2n-1)/2} cos\left(\frac{\left(2n+1\right)\theta}{2}\right) \\
&= \frac{1}{\mu} \left[\ldots\ldots + \underbrace{b_1^{II} \varepsilon^{5/2+\lambda/2}}_{r^{1/2}} cos\left(\frac{3\theta}{2}\right) + \underbrace{b_0^{II} \varepsilon^{3/2-\lambda/2}}_{r^{-1/2}} cos\left(\frac{\theta}{2}\right) + \underbrace{b_0^{II} \varepsilon^{3/2-3\lambda/2}}_{r^{-3/2}} cos\left(\frac{\theta}{2}\right) + \ldots\ldots \right]
\end{aligned} \tag{35}$$

Note that in the second series (35), the $r^{-3/2}$ term is always the dominant term in A' as $\varepsilon \to 0$ which is $\mu^{-1} \varepsilon^{3/2-3\lambda/2}$. Since the stress is the sum of these two series, we must compare the dominate terms of both series, that is:

$$\varepsilon^{-\lambda/2} \text{ and } \mu^{-1} \varepsilon^{3/2-3\lambda/2} \tag{36}$$

Thus, the K field is dominant over all singular and non-singular terms if and only

$$\varepsilon^{-\lambda/2} >> \mu^{-1} \varepsilon^{3/2-3\lambda/2} \Leftrightarrow \varepsilon^{-1+\lambda} \mu \varepsilon^{-1/2} >> 1 \tag{37}$$

Recall (31) where $\mu^2 = C^{-1} \varepsilon$, substituting this expression into (37) and noting that C is a constant of order 1, the condition of K dominance reduces to

$$\varepsilon^{-1+\lambda} >> 1 \tag{38}$$

which is always true for sufficiently small ε (the size of process zone small compare with specimen dimensions) since $\lambda < 1$. Thus, K dominance reduces to the usual statement of SSY (see Rice above).

We can now address the second issue that that specimens must have overlapping regions where the K field is dominant. This condition is satisfied since A' includes all λ in (0,1) so long as (31) and (38) is satisfied. Of course, the smaller the ε , the more accurate is the K field and it is dominant over a larger region. In other words, the region of dominance for specimens with a larger value of $\varepsilon = \varepsilon_1$ is contained in the region of dominance of a specimen with a smaller value of $\varepsilon = \varepsilon_2$.

As a final example, we plot the shear stress $\tau_y(r, \theta = 0) = \tau_\theta(r, \theta = 0)$ directly ahead of the crack tip where the process zone Ω is a traction free hole (the material inside hole is a Jell-O) (see Figure 4 below). This solution is given by (29c). For this case, the local stress intensity factor increases by the amount $\varepsilon K_{III}^{Applied} / (1 - \varepsilon)$.

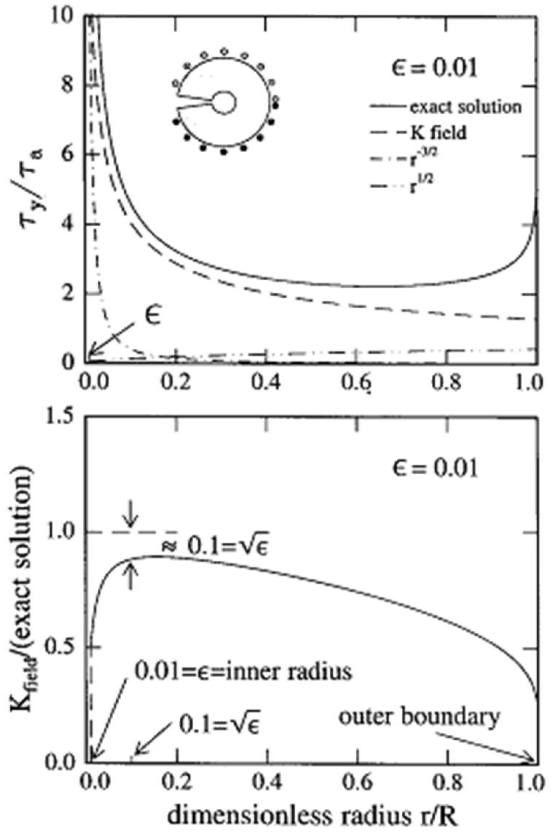

Figure 4a The shear stress τ_y directly ahead of the crack tip is plotted for the case of the traction free hole from $r/R = \varepsilon$ to $r/R = 1$ from the exact solution (29c) (solid line). The applied outer traction is a step function of θ . Also shown are the K field, i.e., the $r^{-1/2}$ term (dash line), the $r^{-3/2}$ term (dotted line) and the $r^{1/2}$ term (dot dot dash) in the series expansion. Note that the $r^{-3/2}$ term is actually larger than the $r^{1/2}$ term for r/R < 0.2. Figure 4b plots the ratio of the K field to the exact solution. This figure shows that the solution for this particular problem is consistent with the general result that the K field is most accurate at r $r \approx \sqrt{\varepsilon} R$ where the fractional error of the K field compare to the exact solution is of order $\sqrt{\varepsilon}$.

Criterion on fracture initiation:

Assuming SSY holds, then the criterion for fracture initiation in Mode I (for sufficiently thick specimens) is

$$K_I = K_{IC} \tag{39}$$

It is important to note that K_{IC} is a material property (sometimes called fracture toughness) that cannot be determined from elasticity analysis. It is determined by testing. The left hand side of the equation is a quantity that is determined by carrying out an elastic calculation accounting for the specimen geometry and the applied load. In a perfectly brittle material when K reaches K_{IC} the crack grows unstable in a load controlled test. However, ductile materials can resist crack growth and requires K > K_{IC} to continue crack growth.

The utility of the SSY concept is important for practical applications such as correlating crack growth rate data in fatigue crack growth and slow growth of cracks under high temperature conditions (creep crack growth). In fatigue crack growth, the applied cyclic loads are typically very small so for sufficiently long cracks, SSY is satisfied[1]. The material behavior in the nonlinear process zone is very complicated (due to repeating loading and unloading, formation of slip bands etc.). However, SSY allows us to conclude that the crack growth rate must be controlled by the elastic K field; therefore, it is the correct parameter to correlate data.

References:

[1] The stress analysis of cracks handbook, 3rd edition: by Hiroshi Tada, Paul C. Paris and George R. Irwin. ASME press.

[2] J.R. Rice, in Fracture, H. Liebowitz (ed.), vol.2 Academic Press, NY (1968), p191.

[3] C.Y. Hui and A. Ruina, Intl. J. Fracture, 72: 97-120, 1995

[4] John W. Hutchinson, "A course on Nonlinear Fracture Mechanics", Department of Solid Mechanics, The Technical University of Denmark, 1979.

[1] Most of the life time of fatigue cracks in real structures can be spend in the regime where the crack is very small, in this regime, SSY is likely to be violated.

Appendix:

The stress near the edge is complicated and was studied first by J. P. Benthem, "State of stress at the vertex of a quarter-infinite crack in a half space", Int. J. of solids & Structures, 1977. Vol. 13. pp. 479. By limiting his analysis to stresses that are symmetrical to the crack plane, he showed that the stress field at the vertex of a quarter-infinite crack in a half space (z > 0), see picture below, has the formed given by

$$\sigma_{ij} = Ar^{\lambda} f_{ij}(\theta,\phi)$$

where (r,ϕ,θ) is a spherical coordinate system with origin at the vertex where the crack intersects the surface of the half space (note that (r,θ) is defined differently in here than in the main text of this lecture) . In figure above, the crack occupies the half plane z > 0, x > 0 and y = 0 with its front along the positive z axis. The order of singularity, λ depends on the Poisson's ratio, for the special case of *v = 0,* $\lambda = -1/2$ *(note* $\sigma_{33} = 0$ *in this case, see (15)).* In general, λ increases with Poisson's ratio, and equals to -0.3318 for the case of an incompressible solid. Thus, the corner singularity is weaker than the square root singularity of the crack tip solution. It can be shown that if one approaches the crack front z > 0 from x < 0, y =0,

$$\sigma_{yy}(-x \to 0^{+}, y = 0, z) \propto \frac{z^{\lambda+1/2}}{\sqrt{|x|}}$$

Since $\lambda < 1/2$ except for Poisson's ratio = 0, the stress intensity factor vanishes as one approaches the crack front from the corner.